Supplementary information for

Flow-through Microfluidic Photoionization Detectors for Rapid and Highly Sensitive Vapor Detection

Hongbo Zhu,[a] Robert Nidetz,[b] Menglian Zhou,[a] Jiwon Lee,[a]

Sanketh Buggaveeti,[b] Katsuo Kurabayashi[b] and Xudong Fan[*a]

[a]Department of Biomedical Engineering, University of Michigan,

1101 Beal Avenue, Ann Arbor, Michigan 48109, United States

[b]Department of Mechanical Engineering, University of Michigan,

2350 Hayward, Ann Arbor, Michigan, 48109, United States

[*]xsfan@umich.edu

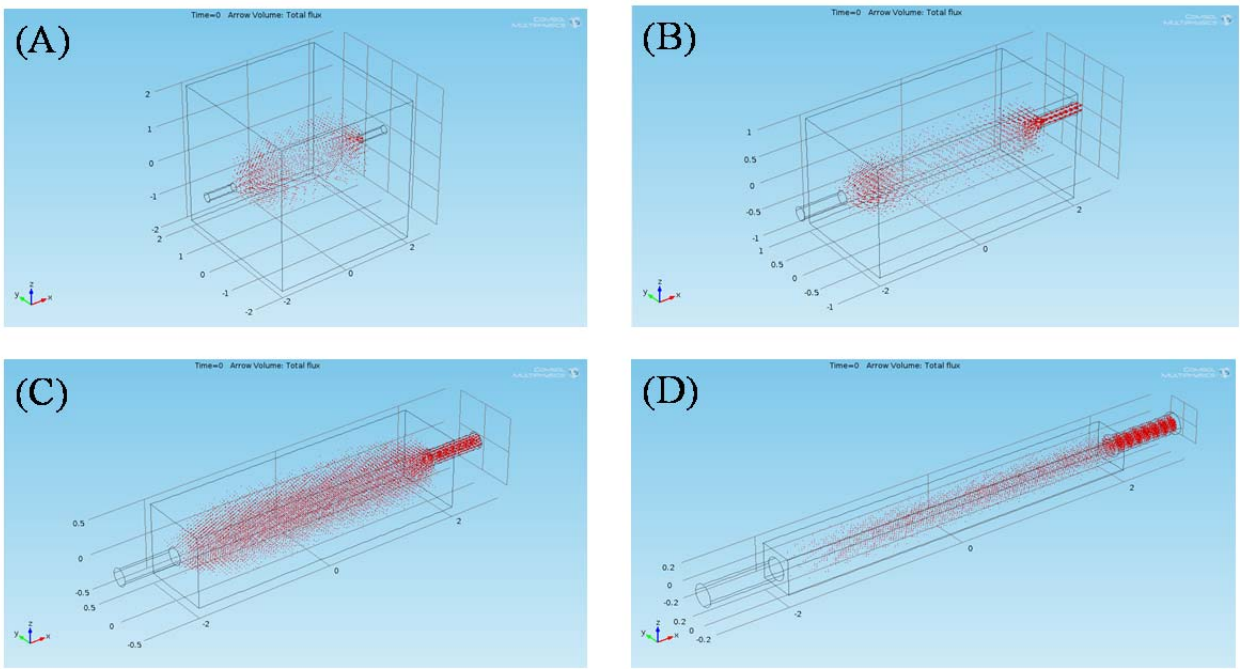

Fig. S1. COMSOL simulation of analyte (toluene) concentration (flux) magnitude for various sizes of chambers. (A) 4x4x4 mm^3 = 64 μL. (B) 2x2x4 mm^3 = 16 μL. (C) 1x1x4 mm^3 = 4 μL. (D) 0.4x0.4x4 mm^3 = 0.64 μL. The inlet and outlet have a diameter of 0.25 mm. Initially, the chamber is filled homogeneously with toluene. Purging gas, helium, is flowed in at t=0 at a flow rate of 5 mL/min to purge the chamber. The dead volume, defined as the region inside the chamber having a helium flow velocity less than 10% of the maximal velocity, is estimated to be 35.7 μL, 6.55 μL, 1.57 μL, and 0.24 μL, respectively, for (A)-(D).

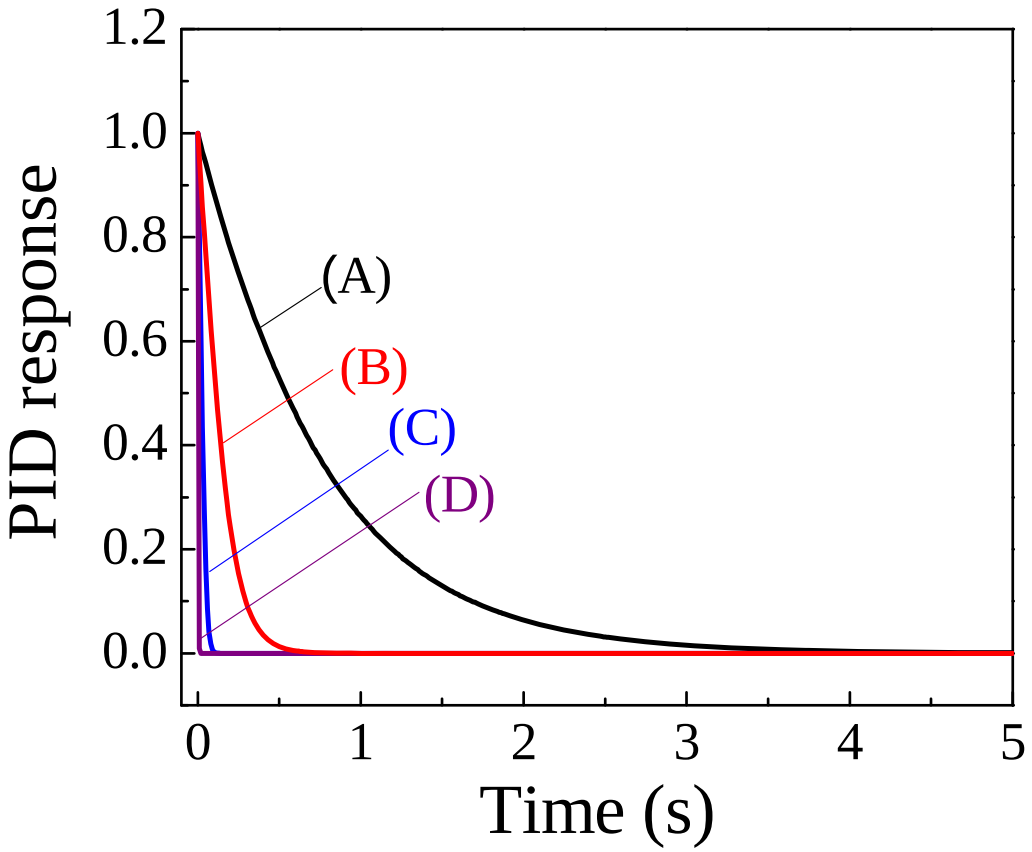

Fig. S2. Normalized PID response (proportional to the volume-averaged toluene concentration inside the chamber) as a function of purging time for various chamber sizes. Curves (A)-(D) correspond to Figs. S1(A)-(D). The fall time (*i.e.*, the time from the peak to 10% of the peak) is 1.69 s, 0.3 s, 0.049s, and 0.0035 s, respectively, for Curves (A)-(D).

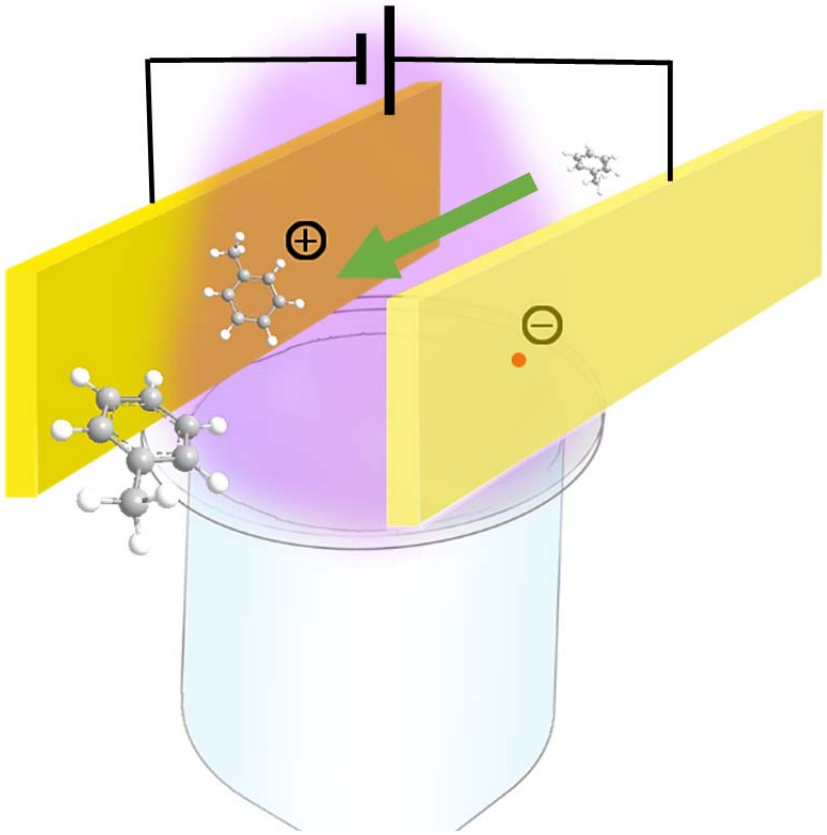

Fig. S3. PID working principle.

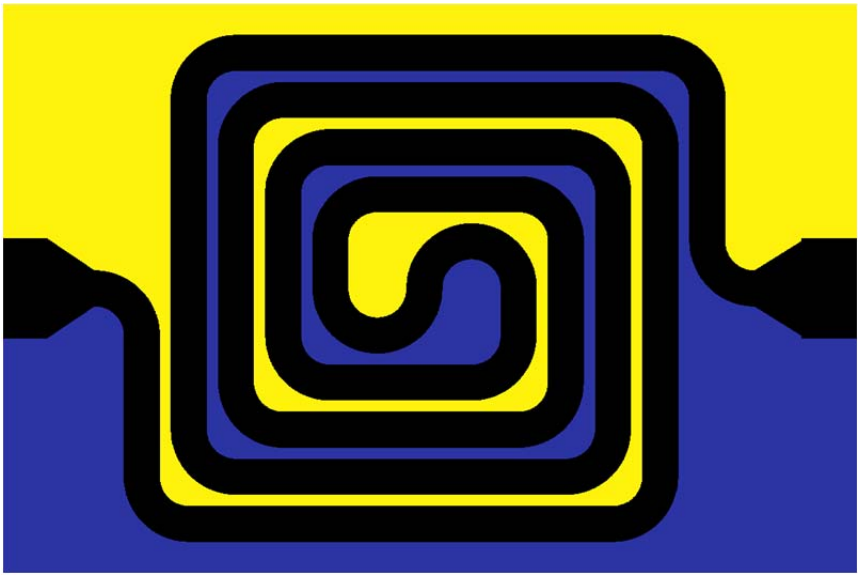

Fig. S4. Electrode layout for the microfluidic PID. Blue and yellow: electrodes. Black: microfluidic channel.

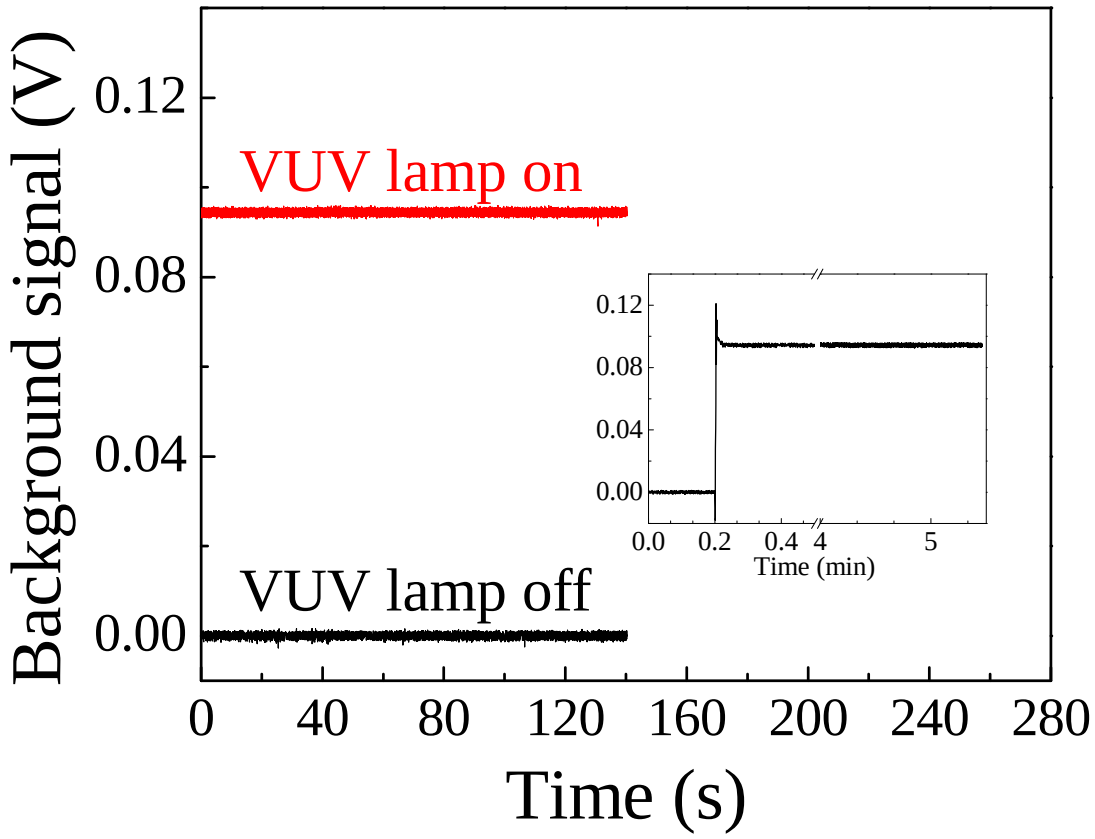

Fig. S5. Voltage signal increases by 94.3 mV when the VUV lamp is turned on, which corresponds to a 94.3 pA current change prior to the amplifier. The standard deviation of the noise is 0.68 mV. Amplification = 10X. Internal resistance of the amplifier = 100 MΩ + 25 pF. During the measurement, helium was flowed through the microfluidic PID at a flow rate of 2 mL/min. Inset shows long-term stability up to 5.5 minutes.

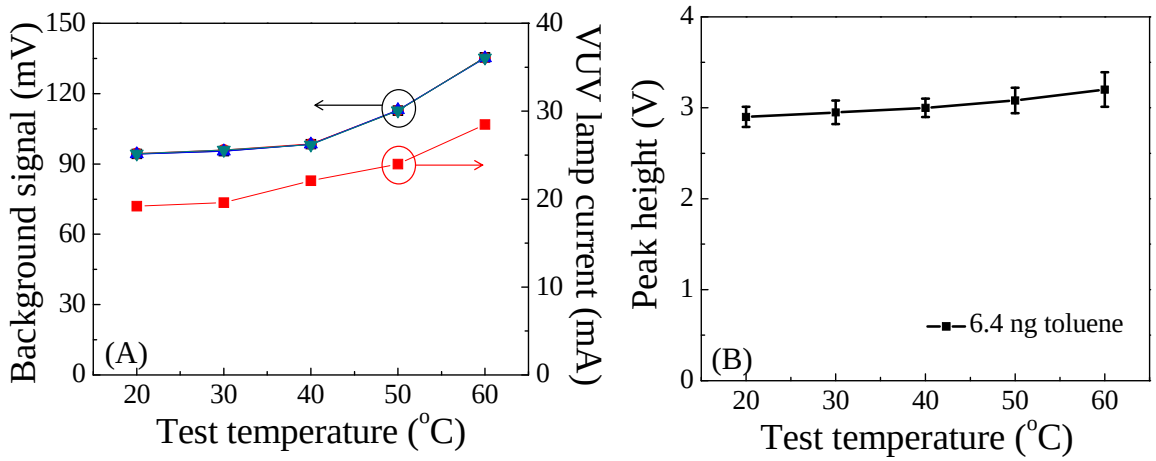

Fig. S6. Microfluidic PID temperature stability tests. (A) Left Y-axis: Baseline signal as a function of device temperature. The noise level remains the same as for 20 °C (Fig. S5). Right Y-axis: Current of the VUV lamp drive circuit. (B) PID sensitivity to analyte as a function of temperature. The corresponding baselines are removed. Error bars are calculated based on 4 measurements. During the test, the entire device was placed inside a GC oven. 60 °C is the maximal operating temperature specified by the VUV lamp manufacturer.

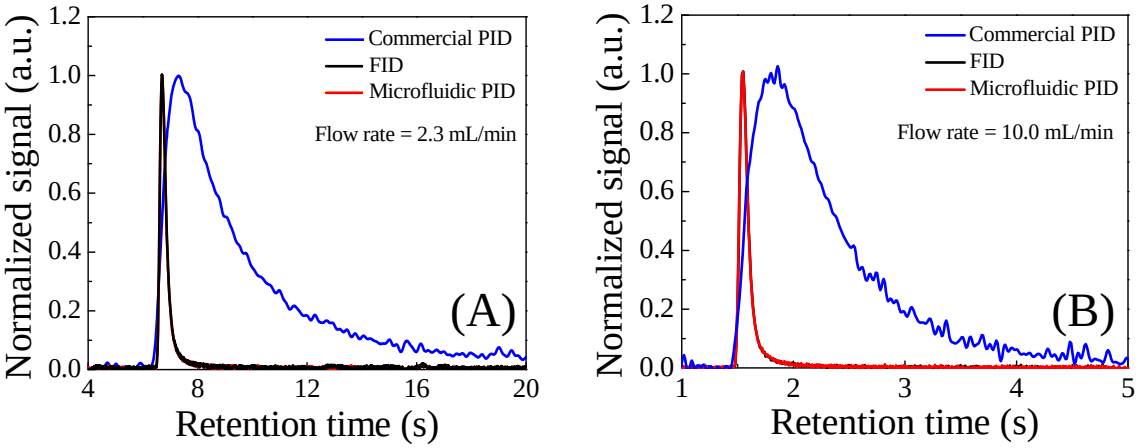

Fig. S7. Normalized toluene peak obtained with commercial PID, FID, and microfluidic PID at the flow rate of 2.3 mL/min and 10 mL/min, respectively. The corresponding magnified curves for FID and microfluidic PID are plotted in Fig. 3.

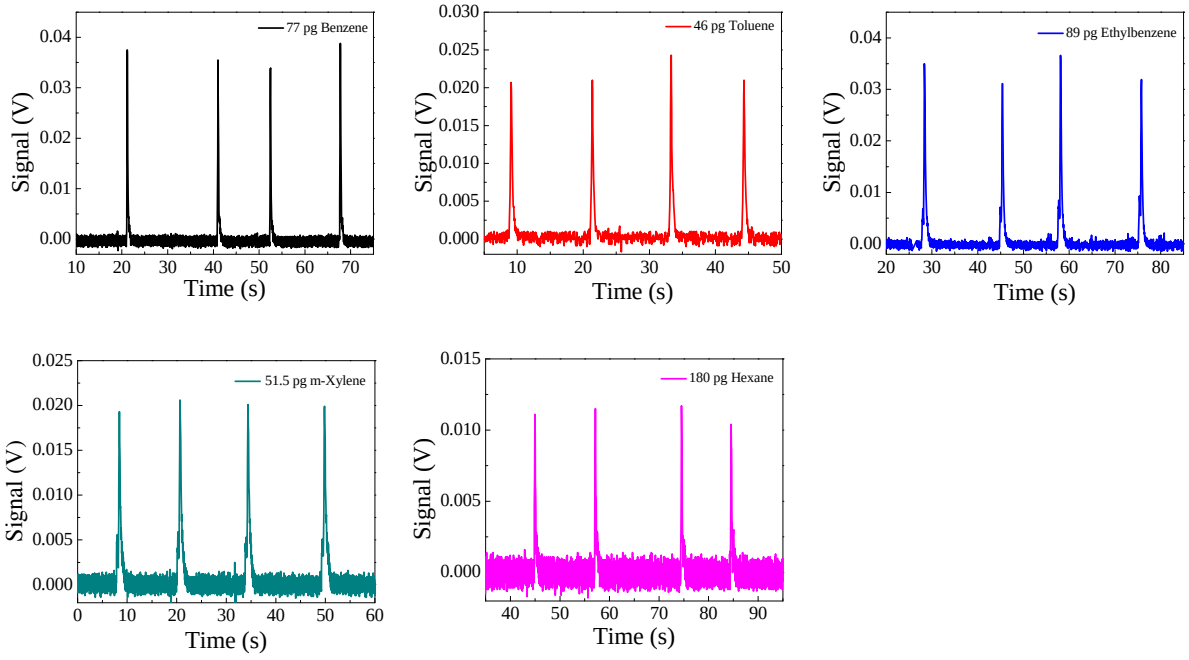

Fig. S8. Microfluidic PID signals for repeatable measurements (4 times) of various analytes that were injected into the GC-PID system.

Table S1. Comparison among micro-PID, plasma-based PID, and microfluidic PID. Red highlights denote meritorious or preferred features.

	μPID (reported in Ref. 1)	**Plasma-based PID (Reported in Ref. 2)**	**Microfluidic PID (this work)**
Design concept	Traditional design concept, but with a smaller chamber volume	New concept with micro-discharge integrated on a chip	New microfluidic flow-through concept. Low chamber volume and dead volume. Large electrode area. Low voltage
Ionization source	UV lamp on top of the ionization chamber (10.6 eV)	UV + Plasma (~20 eV)	UV lamp on top of the ionization channel (10.6 eV)
Discharge electrode degradation	No	No (according to 12-hr continuous testing)	No
Source/analyte contact	Non-contact	Contact	Non-contact
External helium flow required	No	Yes	No
High voltage required	Yes (150 V)	Yes (>500 V)	No (6 V)
Power consumption	~100 mW (mainly for VUV operation)	1.4 mW	~100 mW (mainly for VUV operation)
Detection limit	5 ppb for benzene, toluene, and styrene (no mass detection limit reported)	~10 pg for n-Octane	~5 pg for benzene, toluene, ethylbenzene, and m-xylene
Chamber size	10 μL	Not reported	1.3 μL
Response time (baseline to 90% of the peak)	30 ms for 30 mL/min flow rate	170 ms for 2.5 mL/min flow rate	160 ms and 55 ms for 2.3 and 10 mL/min flow rate, respectively
Dynamic range	6 orders of magnitude	Not reported	6 orders of magnitude
Linearity	Non-linear (square root)	Not reported	Linear
Integration with μGC systems	Acceptable	Best	Better
Temperature stability	Tested (25 ^{o}C)	Tested (40-100 ^{o}C)	Tested (20-60 ^{o}C)
Flow rate stability	Tested (1.5 and 30 mL/min)	Tested (0.9– 2.7 mL/min)	Tested (2.3 – 10 mL/min)
Undesirable negative peaks in signal	Not present	Present (reasons unknown)	Not present

Table S2. Linear curve fit parameters used in Fig. 5(A).

	Benzene	**Toluene**	**Ethylbenzene**	**m-Xylene**	**Hexane**
Slope (Vs per ng)	0.10452	0.07719	0.04908	0.05752	0.01274
R^2	0.9856	0.96264	0.96136	0.9734	0.98119
Molecular weight (g/mol)	78	92	106	106	86
Slope (Vs per mol)	7.8×10^9	7.1×10^9	5.2×10^9	6.1×10^9	1.1×10^9

Transit time calculation

Assuming a uniform electric field, the time for ions to move from one electrode to another, t, is given by

$$t = \sqrt{\frac{2m}{eV}} \cdot L, \quad \text{(S1)}$$

where m and e are the mass and charge of an ion, respectively. L is the distance between the two electrodes. V is the applied voltage.

References

1. J. Sun, F. Guan, D. Cui, X. Chen, L. Zhang, and J. Chen, "An improved photoionization detector with a micro gas chromatography column for portable rapid gas chromatography system," Sens. Actuators B **188**, 513– 518 (2013).
2. M. Akbar, H. Shakeel, and M. Agah, "GC-on-Chip: Integrated Column and Photo Ionization Detector," Lab Chip **15**, 1748-1758 (2015).